JOURNAL OF BACTERIOLOGY, Oct. 2005, p. 6641–6650 Vol. 187, No. 19
0021-9193/05/$08.00+0 doi:10.1128/JB.187.19.6641–6650.2005

Small Untranslated RNA Antitoxin in *Bacillus subtilis*†

Jessica M. Silvaggi,[1] John B. Perkins,[2] and Richard Losick[1]*

Department of Molecular and Cellular Biology, The Biological Laboratories, Harvard University, Cambridge, Massachusetts 02138,[1] and DSM Nutritional Products, Ltd., Biotechnology R&D, P.O. Box 3255, Building 203/20A, CH-4002 Basel, Switzerland[2]

Received 27 May 2005/Accepted 7 July 2005

Toxin-antitoxin (TA) modules are pairs of genes in which one member encodes a toxin that is neutralized or whose synthesis is prevented by the action of the product of the second gene, an antitoxin, which is either protein or RNA. We now report the identification of a TA module in the chromosome of *Bacillus subtilis* in which the antitoxin is an antisense RNA. The antitoxin, which is called RatA (for RNA antitoxin A), is a small (222 nucleotides), untranslated RNA that blocks the accumulation of the mRNA for a toxic peptide TxpA (for toxic peptide A; formerly YqdB). The *txpA* and *ratA* genes are in convergent orientation and overlap by ca. 75 nucleotides, such that the 3′ region of *ratA* is complementary to the 3′ region of *txpA*. Deletion of *ratA* led to increased levels of *txpA* mRNA and lysis of the cells. Overexpression of *txpA* also caused cell lysis and death, a phenotype that was prevented by simultaneous overexpression of *ratA*. We propose that the *ratA* transcript is an antisense RNA that anneals to the 3′ end of the *txpA* mRNA, thereby triggering its degradation.

Toxin-antitoxin (TA) systems are pairs of adjacent genes in which a stable toxic peptide is neutralized by an unstable antitoxin (5). Antitoxins can be either protein or antisense RNA. Several types of bacteria contain toxin-antitoxin systems, which were originally found in extrachromosomal elements, such as plasmids, bacteriophages, and transposons (6). More recently, these modules have also been discovered in bacterial chromosomes, often in multiple copies (7, 26). The majority of the plasmid-borne toxin-antitoxin systems have been detected and studied in *Escherichia coli*, but chromosomal systems are apparently widespread and are found in both gram-negative and gram-positive bacteria (10). A computational search revealed 671 candidates for TA gene pairs in the 126 sequenced bacterial genomes that were investigated (26).

Plasmid-borne toxin-antitoxin systems are often responsible for a process called postsegregational killing. In these systems, when a plasmid producing both the toxin and antitoxin is lost from the cell, the antitoxin, which is characteristically unstable, is quickly degraded, whereas the toxin, which is comparatively stable, persists long enough to kill the resulting plasmid-free cell (27). These types of systems, also known as "addiction modules," ensure that only cells that contain a plasmid are maintained in the population. Diverse functions have been attributed to various plasmid-encoded toxins, including inhibition of DNA gyrase, inhibition of DnaB-dependent replication, and cell membrane depolarization (17). In contrast, chromosomally encoded toxin-antitoxin systems are believed to be beneficial to cell survival by being part of global stress response systems (10). It has been shown that the MazF, RelE, and ChpBK toxins in the *E. coli* chromosome inhibit protein synthesis by inducing cleavage of translated mRNAs during nutrient starvation (7). Therefore, it is thought that inhibition of translation may aid in curtailing the consumption of nutrients during starvation. Another toxin in *E. coli*, HipA, is proposed to be responsible for the persister state in which the bacteria temporarily stop growing and thereby evade the killing effects of antibiotics that block cell wall synthesis (2, 21).

Most chromosomally encoded and plasmid-encoded antitoxins are unstable proteins (7, 12). In general, the antitoxin protein is generated in excess but is less long-lived than the toxic peptide due to degradation by a specific protease (9). Normally, the antitoxin binds tightly to the toxic peptide, preventing it from acting on cellular targets. Well-known examples of such systems in *E. coli* are the *ccd* module of plasmid F, the *kis*/*kid* module of plasmid R1, the *phd*/*doc* module of P1 plasmid, and the chromosomal module *mazEF* (9). Few intracellular targets have been discovered for the plasmid encoded toxins (17), while it has been proposed that chromosomally encoded TA loci enable bacteria to cope with nutritional stress (11).

Some antitoxins are small, untranslated RNAs, and these are generally believed to act as antisense RNAs that pair with the mRNA for the corresponding toxin, thereby inhibiting its translation or promoting its degradation (5), (12). Examples of plasmid-borne TA systems that use antisense RNAs are *hok*/*sok* (12) from plasmid R1 and *flm* from F plasmid (24) in *E. coli* and the *par* locus in plasmid pAD1 in *Enterococcus faecalis* (13). More recently, two examples of chromosomal toxin-antitoxin systems have been identified in *E. coli* that use an antisense RNA as an antidote. One such small, untranslated RNA, IstR, was found to be an inhibitor of the synthesis of an SOS-induced toxic peptide (31) and the other, RdlD, of the synthesis of the toxin LdrD (20).

We are interested in discovering small, untranslated RNAs in the chromosome of *Bacillus subtilis*. In the aforementioned hunt for toxin-antitoxin gene pairs from 126 sequenced prokaryotic genomes, only one putative toxin-antitoxin system, which is similar to the *mazEF* suicide module in *E. coli* (26), was predicted in this spore-forming bacterium. Recently, this

* Corresponding author. Mailing address: Department of Molecular and Cellular Biology, The Biological Laboratories, 16 Divinity Ave., Harvard University, Cambridge, MA 02138. Phone: (617) 495-4905. Fax: (617) 496-4642. E-mail: Losick@mcb.harvard.edu.

† Supplemental material for this article may be found at http://jb.asm.org/.

TABLE 1. Strains and plasmids used in this study

Strain or plasmid	Genotype	Reference, source, or construction
Strains		
B. subtilis		
PY79	Wild type; prototroph	33
JS94	*igr-1*Δ::*tet*	This study
JS178	*igr-2*Δ::*tet*	This study
JS182	*igr-2*Δ::*tet amyE*::pJS19 (*cat*)	pJS19→JS178
JS191	*tpxA*Δ::*spc*	This study
JS192	*yqbM*Δ::*spc*	This study
JS226	*igr-2 txpA*Δ::*tet*	This study
JS228	*igr-2*Δ::*tet amyE*::pJS63 (*cat*)	pJS63→JS178
JS248	*amyE*::$P_{hyperspank}$-*txpA (spc)*	pJS64→PY79
JS251	*igr-2 yqbM*Δ::*tet*	This study
JS348	*amyE*::$P_{hyperspank}$-*txpA* (*spc*) *thrC*::P_{xyl}-*ratA* (*erm*)	pJS98→JS248
JS352	*amyE*::$P_{hyperspank}$-*txpA* (*spc*) *thrC*::P_{xyl}-*307ntRNA* (*erm*)	pJS103→JS248
E. coli DH5α	Cloning host	Laboratory stock
Plasmids		
pDG364	Permits recombination into the chromosome at *amyE* (*cat*)	19
pDG1514	Contains *tet* antibiotic cassette	15
pDG1727	Contains *spc* antibiotic cassette	15
pDG646	Contains *erm* antibiotic cassette	15
pDR111	IPTG-inducible $P_{hyperspank}$ promoter at *amyE* (*spc*)	30
pDG1664	Permits recombination into the chromosome at *thrC* (*erm*)	14
pDR150	Xylose-inducible P_{xylA} promoter at *amyE* (*spc*)	Laboratory stock; 29
pGEM-3Zf(+)	Permits in vitro transcription from SP6 and T7 RNA polymerase promoters (*amp*)	Promega
pBSIIKS(+)	Cloning vector (*amp*)	Stratagene
pJS19	pDG364 with *txpA/yqbM* intergenic region sequence	This study
pJS28	pBSIIKS(+) with *txpA/yqbM* intergenic region sequence	This study
pJS63	pDG364 with *ratA, txpA*, and 90-bp *yqbN*	This study
pJS64	pDR111 with *txpA*	This study
pJS75	pDG1514 with flanking DNA sequence for the *txpA/yqbM* intergenic region	This study
pJS97	pDR150 with *ratA*	This study
pJS98	pDG1664 with EcoRI/BamHI fragment from pJS97	This study
pJS100	pGEM-3Zf(+) with *txpA* and *ratA* overlap region	This study
pJS102	pDR150 with 307-nt small RNA	This study
pJS103	pDG1664 with EcoRI/BamHI fragment from pJS102	This study

antitoxin-toxin operon (*ydcDE*) was verified in vivo, and the toxin YdcE was renamed EndoA due to its similarity in cleavage specificity to the MazF/ChpAK/PemK endoribonuclease family (28). While searching for small, untranslated transcripts encoded within the intergenic regions of the *B. subtilis* genome, we discovered a putative toxin-antitoxin gene pair that encodes a small RNA that we call RatA and a toxic peptide that we designate TxpA. The genes are convergently transcribed and overlap by ca. 75 nucleotides at their 3′ ends. Our evidence is consistent with the idea that RatA is an antisense RNA that binds to, and blocks the accumulation of, the mRNA for the TxpA toxin.

MATERIALS AND METHODS

Growth conditions. Strains were grown at 37°C in Luria-Bertani (LB) or Difco sporulation (DS) medium (16). Ampicillin (100 μg ml^{-1}), chloramphenicol (5 μg ml^{-1}), tetracycline 10 μg ml^{-1}, spectinomycin (100 μg ml^{-1}), and MLS (erythromycin 1 μg ml^{-1} and lincomycin 25 μg ml^{-1}) were added to agar plates where appropriate.

Plasmid and strain construction. Strains and plasmids used for the present study are listed in Table 1. Standard techniques were used for stain construction (16). All plasmids were transformed into *E. coli* DH5α by using standard methods and are listed in Table 1. All PCR products were amplified from chromosomal DNA from strain PY79. Primers used for the generation of PCR products indicated below are listed in Table S1 in the supplemental material. All transformations with cells of *B. subtilis* were carried out by the two-step transformation procedure (16).

To generate the complementation construct pJS19, a PCR fragment containing the *txpA-yqbM* intergenic region sequence was amplified with oligonucleotide primers oJS300 and oJS301, ligated to the EcoRI-HindIII sites of pDG364 to place with fragment between the arms of *amyE* (19), and transformed into JS178 to create JS182. A second complementation construct (pJS63) was generated as described above by PCR amplification of a fragment containing *ratA*, *txpA*, and 90 bp of the upstream gene *yqbN* with oligonucleotide primers oJS425 and oJS426 and ligation to the EcoRI-BamHI sites of pDG364. JS178 was transformed with pJS63 to create JS228.

To generate an IPTG (isopropyl-β-D-thiogalactopyranoside)-inducible construct for *txpA* (pJS64), a fragment containing the open reading frame for *txpA* was amplified with oligonucleotide primers oJS427 and oJS428, ligated to the NheI-SphI site of pDR111 (30) to place the fragment between the arms of the *amyE* gene, and transformed into PY79 to create JS248. To generate a xylose-inducible overexpression construct for RatA (pJS98), a fragment containing the DNA sequence for RatA, excluding the promoter region, was amplified with oligonucleotide primers oJS471 and oJS505 and ligated to the SalI-BamHI sites of pDR150 (29) to create pJS97. Next, the EcoRI-BamHI fragment of pJS97 containing P_{xyl}-*ratA* and *xylR* was ligated to the EcoRI-BamHI site of pDG1664 (14) to place the fragment between the arms of the *thrC* gene to create pJS98. To generate a strain for coinduction of *txpA* and *ratA*, pJS98 was transformed into JS248 to create JS348. As a control, a similar coinduction strain (JS352) was generated as described above by using the DNA sequence for an unrelated small RNA of 307 nucleotides (nt) (unpublished data) rather than RatA. A PCR product was amplified for the 307-nt RNA sequence, excluding the promoter region, by using oligonucleotide primers oJS511 and oJS512. This PCR fragment was ligated to the SalI-HindIII site of pDR150 to create pJS102 for xylose induction of the transcript. The xylose-inducible fragment from pJS102 was moved to the *thrC* locus of pDG1664 as described above to create pJS103 and was transformed into JS248.

To create a plasmid containing a deletion or insertion mutation of the *txpA-yqbM* intergenic region, DNA downstream of the intergenic region was amplified with oligonucleotide primers oJS469 and oJS470 and ligated to the SalI-BamHI sites of pDG1514 (15) to create pJS74. Next, a fragment containing the DNA sequence upstream of the intergenic region was amplified with oligonucleotide primers oJS437 and oJS468 and ligated to the SphI-HindIII sites of pJS74 to create pJS75. pJS75 was sequenced by using oligonucleotide primers oJS456, oJS457, oJS458, and oJS459 to ensure the absence of mutations; linearized with NheI; and transformed into PY79 competent cells to generate JS256.

To create a plasmid template (pJS100) for generating the *txpA* riboprobe by in vitro transcription, a PCR fragment containing the DNA sequence for the ~75-nt overlap region of *txpA* and *ratA* was amplified with oligonucleotide primers oJS508 and oJS509 and ligated to the EcoRI-BamHI sites of pGEM-3Zf(+) (Promega).

Deletion/insertion mutants were created by the technique of long-flanking-homology PCR (32) with the following primers: *igr-1* (JS94) with oJS178, oJS179, oJS186, and oJS187; *igr-2* (JS178) with oJS178, oJS290, oJS186, and oJS187; *txpA* (JS191) with oJS340, oJS341, oJS342, and oJS343; *yqbM* (JS192) with oJS344, oJS345, oJS346, and oJS347; *igr-2 txpA* (JS226) with oJS411, oJS412, oJS413, and oJS414; and *igr-2 yqbM* (JS251) with oJS431, oJS432, oJS433, and oJS434. The source of antibiotic resistance genes used in creating the deletion/insertion mutations were pDG1514 (*tet*), pDG1727 (*spc*), and pDG646 (*erm*) (15). For the creation of deletion/insertion mutants using the tetracycline-resistance cassette from plasmid pDG1514, the resistance gene was inserted in the same 5′ to 3′ direction as the gene to be replaced. In all cases, the deletion/insertion mutations were verified by PCR analysis with chromosomal DNA from each of the strains.

RNA isolation. Samples collected for RNA isolation were immediately mixed with an equal volume of methanol at −80°C. After centrifugation at 4°C for 5 min at 4,000 × *g*, the cell pellets were stored at −80°C. RNA was extracted by a hot acid phenol-TRIzol method as follows. For each sample, three separate 15-ml tubes were prewarmed to 75°C. One contained 3.2 ml of LETS buffer (10 mM Tris-HCl [pH 8.0], 50 mM LiCl, 10 mM EDTA, 1% sodium dodecyl sulfate [SDS]). The second contained 2-ml glass beads (Sigma G-4649) with 2.4 ml of acid-phenol (Sigma P-4682), and the third held 3.2 ml of 5:1 phenol-chloroform (Sigma P-1944). Four 1.5-ml tubes containing 0.7 ml of isopropanol were prepared per sample. Cell pellets were resuspended with 3.2 ml of warmed LETS and added to the tube of hot phenol and beads. After vortexing for 3 min, 2.4 ml of chloroform was added to each, followed by vortexing for 30 s. Samples were centrifuged at 3,200 × *g* for 10 min at 4°C, after which 3.2 ml of aqueous phase was added to the 3.2 ml of hot phenol-chloroform, followed by vortexing for 3 min. Samples were centrifuged again at 3,200 × *g* for 10 min at 4°C, and four aliquots of 0.7 ml of aqueous phase were transferred to the four tubes of 0.7 ml of isopropanol. The tubes were left at room temperature for 10 min, followed by microcentrifugation at 14,000 rpm for 25 min at 4°C. Pellets were washed with 1 ml of 75% ethanol-diethyl pyrocarbonate (DEPC)-treated (diethyl pyrocarbonate) water by centrifugation at 14,000 rpm for 5 min at 4°C. Supernatants were removed, and pellets were resuspended in 20 μl of DEPC-treated water, after which all four tubes were combined for each sample. Then, 1.2 ml of TRIzol was added to each tube, and the tubes were vortexed for 15 s and left at room temperature for 5 min. A total of 0.24 ml of chloroform was added to each tube; tubes were then shaken for 15 s and left at room temperature for 2 min. Samples were centrifuged at 14,000 rpm for 15 min at 4°C, after which 0.7 ml of the aqueous phase was transferred to a 1.5-ml tube containing 0.7 ml of isopropanol; samples were then left at room temperature for 10 min. Tubes were then microcentrifuged at 14,000 rpm for 25 min at 4°C. Pellets were washed with 1 ml of 75% ethanol-DEPC water by centrifugation at 14,000 rpm for 5 min at 4°C. All supernatants were removed, and pellets were air dried for 2 min at room temperature. Pellets were resuspended in 10 to 30 μl of DEPC-treated water, incubated at 55°C for 2 min, and stored at −80°C. Then, 1 μl of each preparation was tested for determination of the optical density at 260 nm (OD_{260})/OD_{280}. Two samples of 0.5 μl were incubated either on ice or at 42°C for 45 min and were run on an agarose gel to check for RNA degradation of the rRNA bands.

Northern blot analysis. After samples were heated for 5 min at 95°C, 5 μg of total RNA in loading buffer (80% formamide, 1 mg of xylene cyanol Ff ml^{-1}, 1 mg of bromophenol blue ml^{-1}, 1× TBE [Tris-borate-EDTA buffer]) was loaded per lane and resolved on 10% polyacrylamide denaturing gels containing 8 M urea. Gels were preheated to ca. 50 to 55°C and run in 1× TBE at ca. 21 to 24 W. After the gel was soaked for 10 min in 0.5× TBE, RNA was transferred at 4°C overnight to Hybond-N nylon membrane (Amersham) at 10 V in 0.5× TBE. Membranes were UV cross-linked with 120,000 μJ/cm^2 (Stratalinker 2400; Stratagene) and blocked for 30 min in 15 to 20 ml of Ultrahyb hybridization buffer (Ambion) at 42°C for double-stranded PCR probes or 68°C for riboprobes. Hybridizations were performed at 42°C (double-stranded probe) or 68°C (riboprobe) overnight for all blots. For the double-stranded probe, membranes were washed with shaking twice with 2× SSC (1× SSC is 0.15 M NaCl plus 0.015 M sodium citrate)–0.1% SDS at room temperature for 5 min and twice with 0.1× SSC–0.1% SDS at 37 to 42°C for 15 min. For the riboprobe, all washes were performed at 68°C. Membranes visualized by phosphorimaging.

Probe labeling. PCR-generated double-stranded probes (oJS99 and oJS100 for RatA detection) were labeled by using the Random Primers DNA Labeling system (Invitrogen) with radiolabeled [α-^{32}P]dCTP (10 mCi ml^{-1}, 3,000 Ci). Excess nucleotides were removed with QIAGEN's Nucleotide Removal Kit, eluting 50 μl. Sheared salmon sperm DNA (200 μl) was added to the probe, and the mixture was boiled for 5 min at 100°C before being added to the membrane (~10^7 cpm).

The *txpA* riboprobe was transcribed by using pGEM-3Zf(+) (Promega) construct (pJS100) and the MAXIscript SP6/T7 in vitro transcription kit from Ambion with [α-^{32}P]UTP (10 mCi ml^{-1}, 800 Ci). Excess nucleotides were removed by using NucAway Spin columns (Ambion). The approximate activity of reaction products was ~10^9 cpm μg^{-1}.

The ladder used was MspI-digested pBR322, end labeled with [α-^{32}P]dCTP (10 mCi ml^{-1}, 3,000 Ci) by using the Klenow fragment.

Primer extension and dideoxy sequencing. (i) Primer labeling. A total of 10 pmol of primer was end labeled with 1 μl of polynucleotide kinase (PNK), 1 μl of 10× PNK buffer, and 4 μl of [γ-^{32}P]ATP in a 10-μl reaction. The reaction was incubated at 37°C for 30 min, after which 40 μl of TE (pH 8.0) was added, and the reaction was cleaned with the QIAquick nucleotide removal kit, eluting 50 μl (1 μl was ~0.2 pmol).

(ii) Primer extension. A total of 10 to 30 μg of RNA was added to 0.2 pmol of end-labeled primer (oJS13 for RatA and oJS466 for *txpA*) and 2 μl of 5× first-strand buffer (Invitrogen SuperScript First Strand Synthesis System for RT-PCR) and brought to a final volume of 10 μl with DEPC water. The RNA mix was annealed to the primer by placing the tube at 95°C for 1 min, transferring to 70°C for 10 min, and ice for 2 min. An extension mix was made up of 5 μl of the above annealing mix, 1 μl of 0.1 M dithiothreitol, 1 μl of 10 mM deoxynucleoside triphosphates (dNTPs), 1 μl of 5× first-strand buffer, and 1 μl of RNase inhibitor. To this mix was added 1 μl of SuperScript II reverse transcriptase, and the reaction was placed at 42°C for 1 h. To stop the reaction, 5 μl of formamide loading buffer (80% [wt/vol] formamide, 10 mM EDTA, 1 mg of xylene cyanol Ff ml^{-1}, 1 mg of bromophenol blue ml^{-1}) was added.

(iii) Dideoxy sequencing ladder. Plasmids (5 μg) containing the appropriate DNA sequence (pJS28 for *ratA* and pJS63 for *txpA*) were alkali-denatured by using 2 μl of 2 N NaOH containing 1 mM EDTA for 10 min at room temperature before adding ammonium acetate to a final concentration of 1 M. The DNA was ethanol precipitated and resuspended in 6 μl of H_2O to which 2 μl of 5× Sequenase reaction buffer (USB) and 0.4 pmol of the end-labeled primer were added. The annealing mix was heated to 65°C for 2 min and cooled at room temperature to <35°C (~30 min) and chilled on ice. To the annealing mix 2 μl of 1.5 μM dNTPs, 1 μl of 0.1 M dithiothreitol, and 3.2 U of Sequenase (USB) were added. The reactions were incubated at room temperature for 2 min, and 3.5-μl portions of the reactions were transferred to tubes prewarmed to 37°C containing 200 pmol of dNTPs, 20 pmol of the appropriate ddNTP, and 50 mM NaCl. After incubation of the termination reactions for 5 min at 37°C, the reactions were stopped by adding 4 μl of formamide loading buffer.

Primer extension and sequencing reactions were incubated at 95°C for 5 min before being loaded on an 8% denaturing sequencing gel containing 7 M urea. A total of 6 μl of primer extension and 3 μl of sequencing reactions were loaded onto a prewarmed gel (ca. 50 to 55°C) and run at 35 to 42 W in 1× TBE. Gels were dried and visualized by phosphorimaging.

DNA sequencing. PCR and plasmid templates for sequencing were purified with QIAGEN QIAquick PCR purification or gel extraction kits. Sequencing reactions were performed by using the ABI Prism BigDye Terminator v1.1 sequencing kit (Applied Biosystems) and analyzed with a Perkin-Elmer ABI Prism 3100 genetic analyzer.

5′- and 3′-RACE PCR. 5′-RACE (rapid amplification of cDNA ends) assays were carried out with 20 μg of total RNA purified from cells grown in DS medium and collected during the exponential phase of growth. 5′ triphosphates were converted to monophosphates with 20 U of tobacco acid pyrophosphatase (TAP) (Epicenter Technologies) at 37°C for 1 h in a total reaction volume of 50 μl containing 1× TAP buffer and 20 U of RNase inhibitor (Roche). Then, 20 μg of control RNA was similarly treated in the absence of TAP. Four units of RNase-free DNase I (Ambion) were added to the reactions, followed by further incubation for 15 min at 37°C. Reactions were stopped by phenol-chloroform extraction, and RNA was precipitated with ethanol and sodium acetate. Pellets were resuspended in 9.5 μl of water, mixed with 500 pmol of a 5′ RNA adaptor JSA3 (Dharmacon Research), denatured at 95°C for 5 min, and quick-chilled on

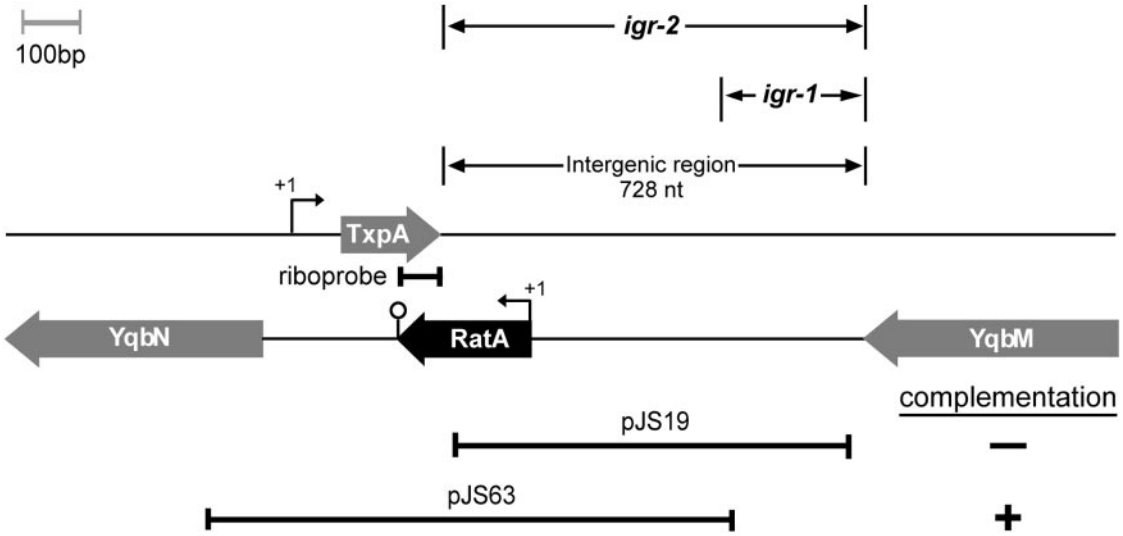

FIG. 1. *txpA-yqbM* intergenic region. Depicted are both DNA strands of the intergenic region and flanking DNA and the orientation and location of *ratA* and protein-coding genes adjacent to the intergenic region. Transcriptional start sites are indicated by +1. A predicted stem-loop terminator is indicated at the end of *ratA*. Also depicted is the riboprobe that was used to detect *txpA* mRNA. Shown at the top are the boundaries of the intergenic region and segments of DNA deleted in the *igr-1* and *igr-2* mutations. Shown at the bottom are segments of DNA used in the complementation analysis with a "+" indicating complementation by the indicated DNA segment and a "–" indicating the absence of complementation.

ice. The adaptor was ligated to the RNA at 16°C overnight with 50 U of T4 RNA ligase (New England Biolabs) in the provided ligase buffer in the presence of 20 U of RNase inhibitor. The RNA was extracted with phenol chloroform and precipitated as described above, and 5-μg aliquots were reverse transcribed with gene-specific primers (10 μM) (oJS519, RatA) and the Thermoscript RT system (Invitrogen) according to the manufacturer's instructions. Reverse transcription was conducted by using three 20-min incubations at 45, 55, and 65°C and a final incubation for 5 min at 85°C. The reactions were then incubated for 20 min at 37°C with 1 μl of RNase H. Amplification of the products of reverse transcription (2 μl) was carried out in a 50-μl reaction containing 1× *Taq* buffer (−$MgCl_2$), 10 pmol of each gene-specific (oJS520, RatA) and adaptor-specific primer (oJS517), 12.5 nmol of each dNTP, 2.5 U of Platinum *Taq* DNA polymerase (Invitrogen), and 75 nmol of $MgCl_2$. Cycling conditions were as follows: 94°C for 2 min and then 30 cycles of 94°C for 30 s, 55 to 58°C for 1 min, and 72°C for 2 min, with a final extension at 72°C for 10 min. PCR products were separated in 1.5% agarose gels, and bands of interest were excised, purified with the QIAquick gel extraction kit (QIAGEN), and cloned into pCR2.1 TOPO vector (Invitrogen). Plasmids from the transformants were purified by using the Qiaprep Spin miniprep kit (QIAGEN) and screened for the presence of inserts of the appropriate size by restriction digestion. Plasmids containing inserts were sequenced by using the ABI Prism BigDye Terminator v1.1 Sequencing Kit (Applied Biosystems) with the primers M13 forward and M13 reverse and analyzed with a Perkin-Elmer ABI Prism 3100 genetic analyzer. 3′-RACE assays were conducted with 20 μg of total RNA that had been dephosphorylated with 300 U of bacterial alkaline phosphatase (BAP; Fermentas) at 60°C for 1 h in a total reaction volume of 30 μl containing 1× BAP buffer and 20 U of RNase inhibitor. The reactions were stopped at 50°C for 10 min with 1 μl of 0.5 M EDTA. The RNA was extracted with phenol-chloroform and precipitated as described above. Pellets were resuspended in 9.5 μl of water, mixed with 500 pmol of 3′ RNA adaptor JSE1 (Dharmacon Research), denatured at 95°C for 5 min, and quick-chilled on ice. The adaptor was ligated to the RNAs as described above, phenol-chloroform extracted, and ethanol precipitated, and the pellet was resuspended in 9 μl of water for reverse transcription (20 μg of RNA). Reverse transcription was carried out as described above with a primer complementary to the 3′ RNA adaptor sequence (JS518). Amplification of 4 μl of the reverse transcription products was conducted as described above with a gene-specific primer (oJS521 [RatA] and oJS529 [*txpA*]) and JS518. Cloning and sequence analysis were conducted as described above. Primers and oligonucleotides are listed in Table S1 in the supplemental material.

***txpA* and *ratA* induction experiments.** Strain JS348 was grown in LB broth at 37°C until it reached exponential phase (OD_{600} of ca. 0.5 to 0.6), at which time the culture was split and the inducer(s) were added to appropriate culture at the correct final concentration (130 mM xylose and 100 μM IPTG). For the xylose and IPTG coinduced cultures, both inducers were either added simultaneously during exponential phase or the first inducer was added during exponential phase and incubated for 60 min, after which the second inducer was added. At each time point the OD_{600} was measured, and samples were diluted in LB and spread on LB agar for viability counts after growth at 37°C overnight.

Conservation of RatA and TxpA. The RatA intergenic region and full-length RNA were queried by using nucleotide-nucleotide BLAST from NCBI (http://www.ncbi.nlm.nih.gov/BLAST/). The TxpA protein sequence was searched by using protein-protein BLAST and the BLAST search for short, nearly exact protein sequence matches.

RESULTS AND DISCUSSION

Detection of RNAs from the intergenic region between *txpA* and *yqbM*. In a search for RNAs that originate from the intergenic regions of the *B. subtilis* genome, a transcription signal was detected, using Affymetrix microarrays (23) from the 728-nt interval between the uncharacterized genes *yqdB* (hereafter referred to as *txpA* for reasons explained below) and *yqbM* (Fig. 1). This intergenic region is located within *skin*, a 48-kb genetic element that is excised late in sporulation to produce an intact coding sequence for the transcription factor σ^K (22). To characterize the transcripts from this intergenic region, Northern blot analysis was carried out with RNA isolated from cells during growth and sporulation in DS medium. Five principal transcripts were detected ranging in size from ~307 nt to ~130 nt (Fig. 2A) when the Northern blot was hybridized with a double-stranded DNA probe corresponding to the intergenic region. All of the transcripts appeared to be produced during growth, except for the smallest transcript (130 nt), which appeared at hour 2 of sporulation (Fig. 2A). The use of strand-specific RNA probes revealed that the 307- and 217-nt transcripts were expressed from the upper strand in Fig. 1 (that is, were transcribed to the right), whereas the 130-, 190-,

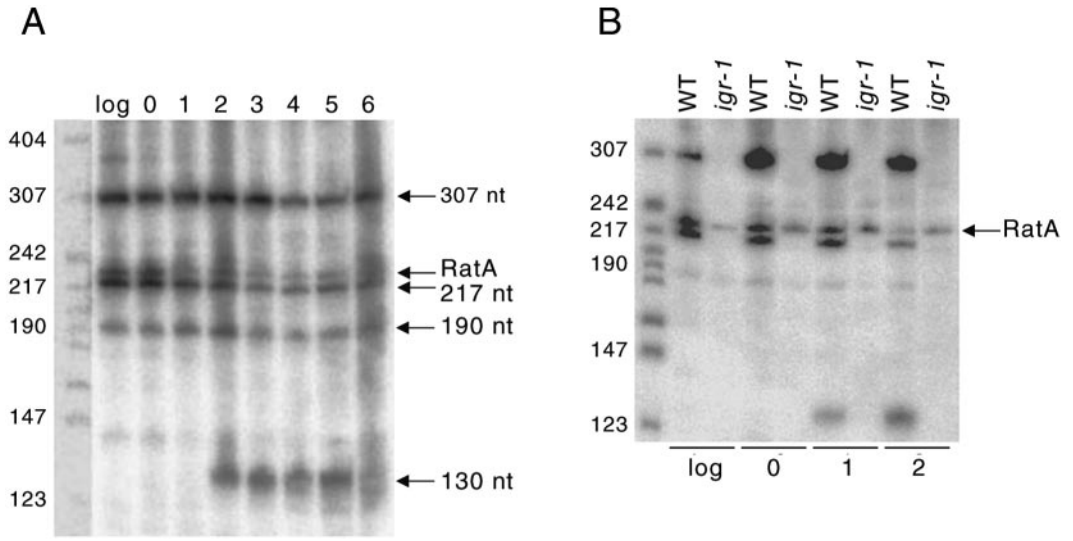

FIG. 2. Detection of RatA by Northern blot analysis. Panel A shows the results with total RNA (5 μg) from wild-type cells grown in DS medium at 37°C and collected during the exponential phase of growth (log) and at hourly intervals during sporulation. Panel B shows the results with RNA from wild-type cells (WT) and *igr-1*-containing cells grown in DS medium and collected during the exponential phase of growth and at hours 0, 1, and 2 of sporulation. The blots of panels A and B were probed with a PCR-amplified, double-stranded DNA that corresponded to the full-length, intergenic region between *txpA* and *yqbM*. Shown on the left of the blots as molecular weight markers are 5′-end-labeled MspI fragments of pBR322 DNA that had been denatured.

and 222-nt transcripts originated from the lower strand (data not shown).

To dissect the region between *txpA* and *yqbM*, a deletion/insertion mutation (*igr-1*) was created in which approximately one-third of the intergenic interval that was closest to *yqbM* was replaced with a tetracycline resistance cassette (Fig. 1). When subjected to Northern blot analysis, RNA from cells of the *igr-1* mutant was found to lack the 307-, 217-, and 130-nt RNAs but to retain the ~230-nt transcript (and reduced levels of the 190-nt species) (Fig. 2B). We conclude that the ~230-nt transcript (and possibly the 190-nt species) originated in whole or in part from the right-hand portion of the intergenic region. Henceforth, we focus our attention on the ~230-nt RNA, which we named RatA (for RNA antitoxin A for reasons explained below). To map the 5′ end of RatA, we carried out primer extension experiments with an oligonucleotide with complementarity to the 230-nt RNA (Fig. 3A). The results revealed a single extension product that defined an apparent start site for a promoter recognized by RNA polymerase containing the housekeeping sigma factor σ^A. The apparent start site was located at an appropriate distance downstream of a perfect match (TGTTATAAT) to a canonical "extended −10" sequence (TGNTATAAT) and a relatively poor match (ATATAA, representing an 2 out of 6 match) to a canonical "−35" sequence (TTGACA) (18). Counting from the edge of the traditional, hexameric −10 sequence (TATAAT), the −10 and −35 sequences were separated from each other by an appropriate spacing of 17 bp.

As evidence that the 5′ end detected for RatA by primer extension was indeed the initiation site rather than a processing site from a longer, primary transcript, we conducted 5′-RACE (rapid amplification of cDNA ends) with the use of TAP enzyme (1, 3) (see Materials and Methods). TAP converts the 5′ triphosphate at the initiating nucleotide of an RNA chain to a monophosphate. Such a monophosphate terminus is required for the subsequent ligation of an RNA adaptor, which, in turn, is needed for reverse transcription and PCR amplification. Thus, PCR amplification products whose synthesis is dependent upon prior TAP treatment of the RNA can be considered to have arisen from transcripts whose 5′ terminus is the initiating nucleotide. Using 5′-RACE the transcriptional start site was mapped to the "A" located 1 nt downstream of that that had been predicted by primer extension (data not shown).

Finally, and reinforcing the view that this is indeed a functional promoter, purified σ^A-containing RNA polymerase generated runoff transcription products from DNA templates containing this promoter that corresponded in size to the start site that had been mapped in vivo (data not shown).

In an attempt to map the 3′ end of the full-length RatA transcript, we conducted 3′-RACE in which an RNA adaptor is ligated to the 3′ end of the RNAs for use in reverse transcription, after which PCR amplification is performed with adaptor- and gene-specific probes. The longest product so obtained contained a 3′ end located 222 nt downstream of the +1 site determined by 5′-RACE, which approximately matched the size of ~230 nt that had been estimated from Northern blot analysis (data not shown). This 3′ end was located after a stretch of uridines that followed a putative rho-independent transcriptional terminator (ΔG −16 kcal/mole). Henceforth, we refer to the size of RatA as 222 nt. Several shorter transcripts of 113, 121, and 136 nt in length were also detected by 3′-RACE.

To test further whether RatA is an untranslated RNA, we searched for open reading frames in which a putative initiation codon (ATG, TTG, or GTG) was preceded at an appropriate distance by a ribosome-binding site. The longest open reading frame that began with a potential initiation codon (ATG) was

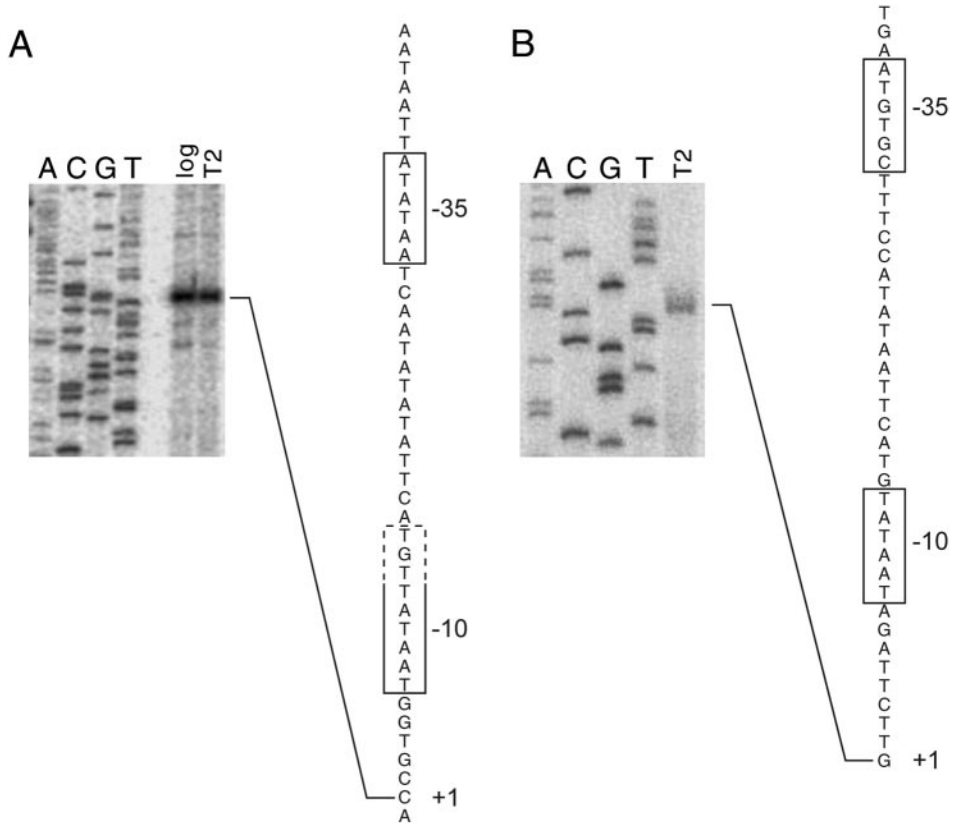

FIG. 3. Mapping the 5′ ends of RatA and *txpA* mRNA. (A) Primer extension experiment with 20 μg of total RNA from wild-type cells grown in DS medium and collected during the exponential phase of growth (log) and at hour 2 of sporulation (T2). The RNAs were used as a template for extension with an end-labeled primer (oJS13) corresponding to *ratA*. A, C, G, and T indicate the dideoxy sequencing ladders generated with the same primer and terminated with the corresponding ddNTP. The corresponding cDNA sequence was determined from the DNA sequencing ladder. The "+1" indicates the 5′ end of the message. The boxes indicate putative −10 and −35 sequences. The dotted portion of the lower box indicates an extended −10 sequence. (B) Primer extension experiment similar to that of panel A except with an end-labeled primer corresponding to *txpA* (oJS466).

only 12 codons in length, and it was not preceded by a sequence that resembled a ribosome-binding site. Thus, it is unlikely that RatA encodes a protein product.

Phenotype of a mutant lacking RatA. The *igr-1* mutation described above caused no conspicuous phenotype and hence failed to provide a clue to the function of the four transcripts that were eliminated by the mutation. To investigate a function for RatA, we created an additional mutation called *igr-2* in which the entire intergenic region was replaced by a tetracycline resistance cassette (Fig. 1). As in the case of the *igr-1* mutant, cells harboring the *igr-2* mutation were created by transformation of wild-type cells with a PCR product that contained the insertion/deletion mutation (see Materials and Methods). When grown as colonies on solid medium containing LB or DS medium, the transformants initially formed normal-looking colonies. However, after several days of growth, many but not all of the colonies exhibited a conspicuous lysis phenotype. As we explain below, the colonies that did not exhibit a lysis phenotype (and indeed those that did) had acquired extragenic suppressor mutations. No lysis phenotype was observed for colonies arising from transformants harboring the *igr-1* mutation.

Northern blot analysis was carried out with RNA from one such *igr-2*-containing mutant that exhibited the colony lysing phenotype. As expected, RNA from the mutant lacked the 222-nt RatA RNA, as well as the 307-, 217-, 190-, and 130-nt RNAs (data not shown).

Together, these observations raise the possibility that the absence of RatA was responsible for the lysis phenotype. Alternatively, the *igr-2* mutation might have caused a polar effect on the expression of an adjacent protein-coding gene. To investigate this possibility, we created null mutants of the flanking genes, *txpA* and *yqbM*, but both mutants were found to form normal-looking colonies that exhibited little lysis after prolonged incubation (data not shown). We also considered the possibility that the lysis phenotype was due to an unknown idiosyncratic feature of the replacement of the intergenic region with a tetracycline resistance cassette. We therefore rebuilt the deletion by reversing the orientation of the cassette and by using an erythromycin antibiotic cassette instead of the tetracycline resistance cassette (data not shown). The phenotypes of mutants containing these alternative deletion/insertion mutations were indistinguishable from those of cells harboring the *igr-2* mutation.

Reversing the colony lysis phenotype by complementation. As a direct test of the idea that the colony lysis phenotype was

caused by the absence of RatA, we attempted to reverse the mutant phenotype caused by the *igr-2* mutation by providing the *ratA* gene in *trans*. Initially, we introduced a copy of the entire intergenic region (contained in pJS19; Fig. 1) into the chromosome at the *amyE* locus in the *igr-2* mutant strain JS178. Colonies from the resulting strain (JS182) remained prone to undergo lysis after several days of incubation. Given that the transcription start site for *ratA* is 147 bp from the left-hand end of the intergenic region and that RatA is about 222 nt in length, *ratA* must extend into the adjacent *txpA* gene by about 75 nt. Hence, the complementation construct we had used (the intergenic region, Fig. 1) would have contained a truncated *ratA* gene. Therefore, we created a second complementation construct (pJS63; Fig. 1) that included the *txpA* coding region, as well as 90 bp of the upstream gene *yqbN*. This construct was expected to contain the entire *ratA* gene and was introduced into the *igr-2* mutant strain JS178. The resulting complementation strain (JS228) did not exhibit a colony lysis phenotype and behaved similarly to the wild type (Fig. 4B). We conclude that the absence of RatA is responsible for the colony lysis phenotype and that the region of *ratA* that extends into, and overlaps with, the convergently oriented *txpA* gene is essential for RatA function.

Mutants lacking RatA accumulate suppressor mutations in *txpA*. As noted above, transformation with *igr-2*-containing DNA or with other mutations removing the intergenic region yielded two kinds of transformants: those that exhibited a conspicuous colony lysis phenotype and those that did not. We reasoned that removal of the intergenic region had selected for transformants (pseudorevertants) that had acquired suppressor mutations that eliminated the toxic effect of the absence of RatA. When chromosomal DNA was prepared from such putative pseudorevertants and used to transform wild-type cells with selection for the drug resistance gene associated with the deletion/insertion mutation, all of the colonies from the resulting transformants failed to exhibit a colony-lysing phenotype. We conclude that the pseudorevertants had acquired suppressor mutations that were located in very close proximity to the intergenic region. In other words, the deletion mutations and the suppressor mutations appeared to cotransform with frequencies approaching 100%. When examined by nucleotide sequence analysis, DNA from the pseudorevertants was found to contain mutations in the 59-codon *txpA* gene. A wide variety of mutations were observed, including several missense mutations and two frameshift mutations (Fig. 4C). These results suggested that *txpA* encoded a toxic peptide and that production of the toxin was prevented by RatA. Even strains that had retained the colony-lysing phenotype were found to harbor mutations in *txpA*, which we interpret as being partial suppressor (partial loss-of-function) mutations.

Because *igr-2* was introduced into *B. subtilis* by transformation with PCR-amplified DNA, we wondered whether the suppressor mutations had arisen spontaneously after transformation or were generated during PCR-mediated amplification. To distinguish between these possibilities, we cloned DNA containing *igr-2* in *E. coli*, verified that the cloned DNA was not mutant for *txpA*, and used the cloned DNA to transform *B. subtilis*. Once again, the resulting transformants were found to have acquired mutations in *txpA*.

As a direct test of the idea that suppression was due to the loss of *txpA* function, we created an *igr-2* Δ*txpA* double mutant (JS226) and, as a control, a *igr-2* Δ*yqbM* (JS251) double mutant. Colonies of the JS251 mutant exhibited the usual colony lysis phenotype, whereas colonies from JS226, which lacks both *txpA* and *ratA*, yielded normal-looking colonies that failed to undergo lysis (Fig. 4B). We conclude that absence of *txpA* reverses the toxicity caused by the absence of *ratA* and hence that *txpA* encodes a toxic peptide.

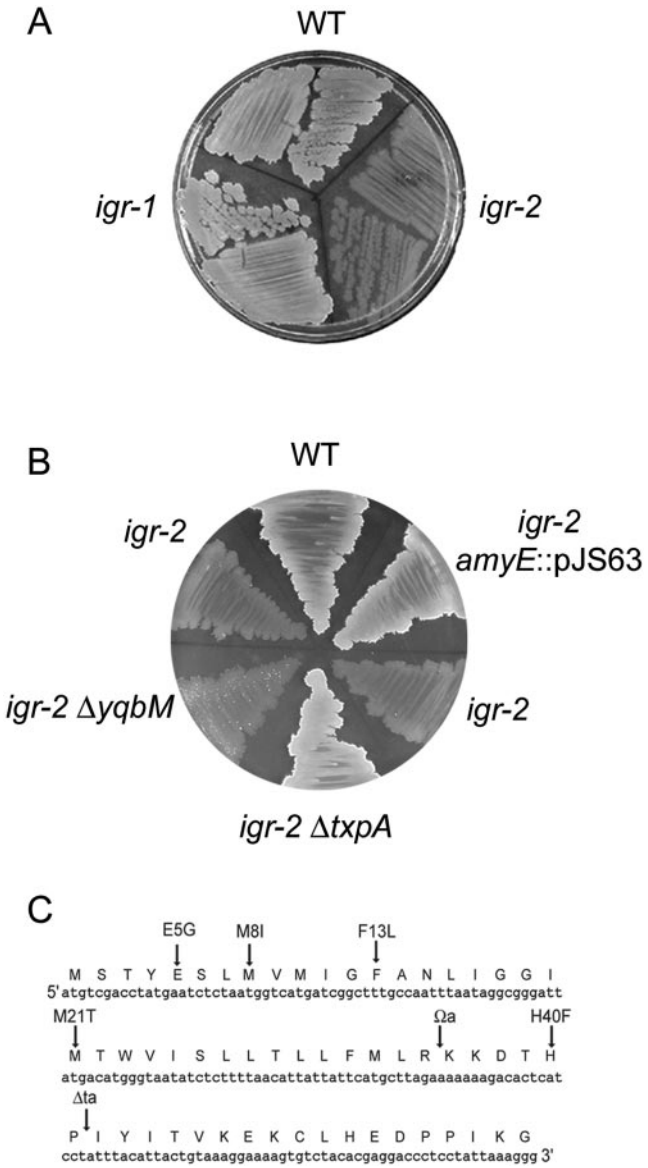

FIG. 4. Complementation of the lysis phenotype caused by the absence of RatA. (A) LB agar plate streaked with the wild type (WT) and with mutants harboring the *igr-1* or *igr-2* mutations and grown at 37°C for 5 days. (B) LB agar plate streaked with the wild type (WT) and with mutants harboring *igr-2* (JS178), *igr-2 amyE*::pJS63 (JS228), *igr-2* Δ*yqbM* (JS251), and *igr-2* Δ*txpA* (JS226) and grown at 37°C for 5 days. (C) Nucleotide and amino acid sequence for *txpA*. Indicated above the amino acid sequence are alterations due to suppressor mutations that arose in transformants generated by transformation with constructs containing deletion/insertion mutations of the *txpA-yqbM* intergenic region.

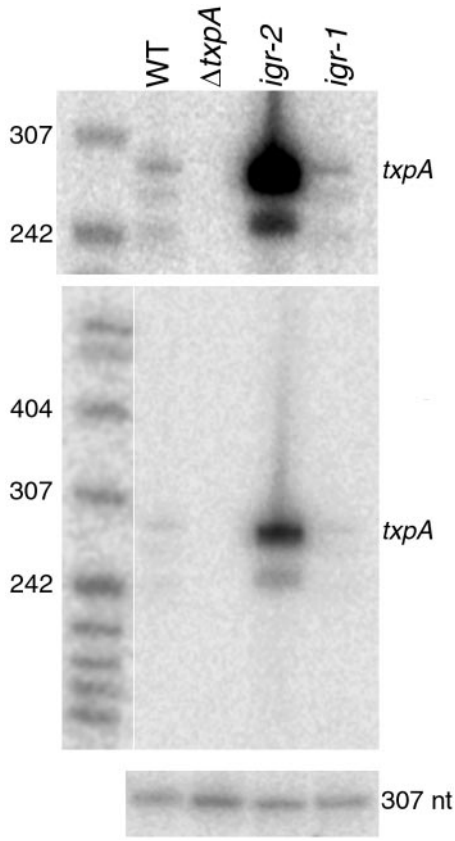

FIG. 5. Visualization of *txpA* mRNA by Northern blot analysis. Total RNA (5 μg) was isolated from wild-type cells (WT) and from cells containing Δ*txpA* (JS191), *igr-2* (JS178), or *igr-1* (JS94) that had been grown in DS medium at 37°C and collected during late exponential growth. The *txpA* transcript was detected by using the riboprobe depicted in Fig. 1, which was complementary to the 3′ end of *txpA*, representing the 75-nt region of overlap with RatA. The upper panel represents a threefold longer exposure of the middle panel for better visualization of the low level of *txpA* mRNA in the wild type. The bottom panel is a loading control probed with a double-stranded probe for an unrelated RNA of 307 nt. The molecular weight markers are 5′-end-labeled MspI fragments of pBR322 DNA that had been denatured.

RatA inhibits the accumulation of *txpA* mRNA. Primer extension analysis revealed a 5′ terminus that was located 48 nt upstream of the *txpA* open reading frame (Fig. 3B). The apparent start site appeared to correspond to a promoter recognized by σ^A-containing RNA polymerase in that it was preceded by a perfect match to a canonical −10 sequence and a weak match (ATGTGC) to a canonical −35 sequence at an optimal spacing of 17 bp between the sequences (Fig. 3B). Northern blot analysis with a riboprobe (Fig. 1) complementary to the portion of the *txpA* mRNA that was antisense to the RatA transcript revealed a constitutively expressed primary transcript of ~275 nt, which likely corresponds to the full-length *txpA* mRNA, and some smaller transcripts that likely represented degradation products (Fig. 5).

Next, we carried out 3′-RACE to determine more precisely the length of the *txpA* transcript and to also look for putative degradation products formed by an interaction with RatA. These experiments revealed a 3′ terminus that was located 247 nt (position +247) downstream from the predicted start site (+1 site; data not shown). We also detected 3′ termini at nucleotide positions +170 and +60. The 170-nt transcript correlated well in size with a species that had been observed by Northern blot analysis (data not shown). The 3′ end for the 170-nt transcript was located close to (within 15 to 20 nt) the 3′ end observed for RatA. An appealing interpretation of these observations is that the 3′ regions of the *txpA* mRNA and of RatA anneal to each other to form a stretch of double-stranded RNA of ca. 75 nt. We hypothesize that this double-stranded region is rapidly degraded in vivo, leaving a single-stranded, truncated *txpA* transcript of about 170 nt. Thus, we interpret the 170-nt RNA as being a degradation product resulting from the interaction of RacA with the *txpA* mRNA.

Next, we examined the effect of RatA on *txpA* mRNA levels. As a control, Fig. 5 shows that *txpA* mRNA was absent in RNA from cells of a Δ*txpA* mutant. Conversely, *txpA* mRNA levels were not significantly altered in RNA from an *igr-1* mutant in which all RNAs from the intergenic region were eliminated except RatA (Fig. 5). In RNA from an *igr-2* mutant, which lacks the promoter and 5′-proximal region of *ratA*, the level of full-length *txpA* mRNA was dramatically higher than that seen in the wild type (Fig. 5). The simplest interpretation of these results is that RatA is an antisense RNA that interferes with the accumulation of *txpA* mRNA by annealing to the mRNA in the region of overlap. We propose that this RNA-RNA interaction causes degradation of *txpA* mRNA.

Overexpression of *txpA* causes cell death. As a further test of the idea that TxpA is a toxic peptide, we created a strain (JS348) in which *txpA* was under the control of an IPTG-inducible promoter and *ratA* was under the control of a xylose-inducible promoter. Figure 6A and B show that the addition of IPTG to cells of strain JS348 growing in liquid medium caused growth to stop abruptly as judged from the drop in the OD of the culture and a precipitous (~10^4-fold) decline in the number of viable cells (Fig. 6A and B). The bactericidal effect of inducing *txpA* was prevented by adding xylose to the culture an hour before IPTG (Fig. 6C and D). When xylose and IPTG were added simultaneously, only a small decrease in OD and the number of viable cells was observed (Fig. 6C and D). Finally, when synthesis of RatA was induced after the induction of *txpA*, little or no protective effect of the antisense RNA was seen (Fig. 6C and D). As a control, a strain was constructed that harbored the IPTG-inducible *txpA* construct and a construct in which the gene for an unrelated small, untranslated RNA was under the control of the xylose-inducible promoter. Prior induction of the synthesis of this heterologous RNA provided no protective effect from the subsequent induction of TxpA synthesis (data not shown). Thus, the protective effect of RatA was not exhibited by another unrelated RNA.

These findings reinforce the view that TxpA is a toxic peptide and raise the question of how it acts. TxpA is not significantly similar to other proteins of known function in the databases, but its first 17 amino acids exhibit 64% identity to a protein of unknown function (orf1, accession AAB09027) of 38 residues from the temperate bacteriophage phi-3T. Also, like the phage protein, TxpA exhibits a putative transmembrane domain in its N-terminal region. We speculate that TxpA acts at the cell membrane, where it damages the integrity of the membrane or, like the amurins of certain bacteriophage (4), it

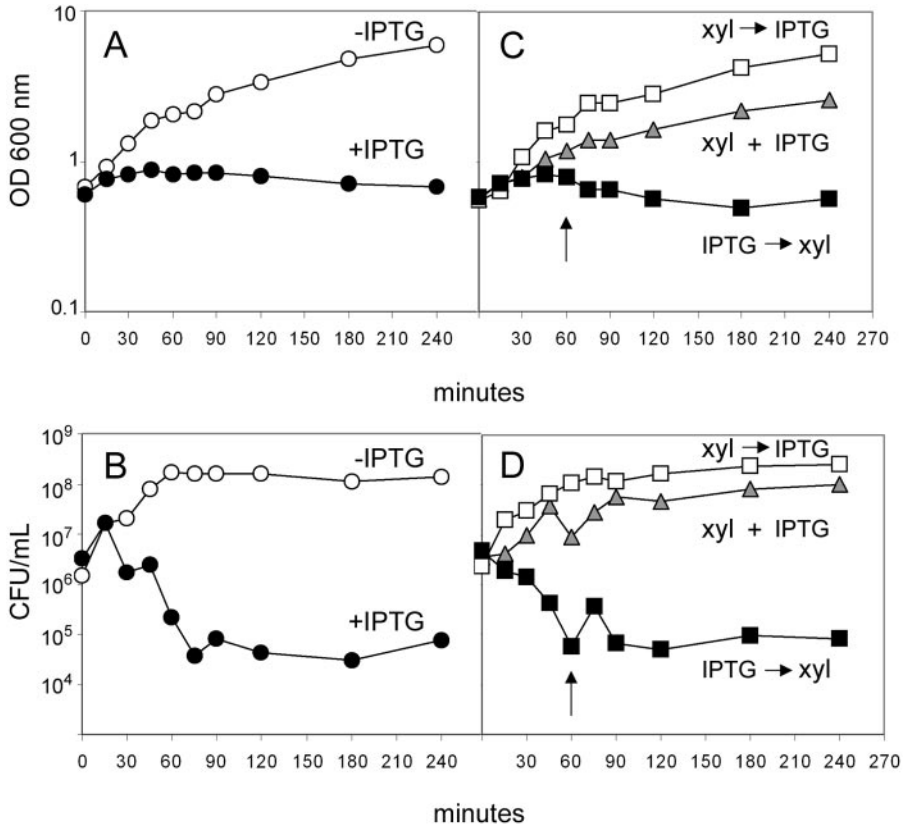

FIG. 6. Induction of *txpA* in the absence of RatA causes cell death. Panels A and C show OD measurements, and panels B and D show measurements of CFU. The experiment was carried out with a strain (JS348) in which *ratA* was under the control of a xylose-inducible promoter and *txpA* was under the control of an IPTG-inducible promoter. Panels A and B show the results for an experiment in which cells at the exponential phase of growth in LB medium at 37°C were split into two cultures, one of which was supplemented with 100 μM of IPTG (●) and the other was not induced (○). Time represents minutes after the addition of inducer. Panels C and D show the results for an experiment in which cells at the exponential phase of growth in LB medium were split into three cultures. One culture was treated simultaneously with 130 mM xylose and 100 μM IPTG (▲) at time zero. The second culture was treated with xylose at time zero and then with IPTG at 60 min as indicated by the arrow (□). The third culture was treated with IPTG at time zero and then with xylose at 60 min (■).

blocks cell wall synthesis. Interestingly, TxpA did not kill cells of an *E. coli* strain that was engineered to produce the *B. subtilis* peptide (unpublished results). Whatever its mode of action, TxpA is evidently not a broad-spectrum toxin.

RatA function does not depend on the Hfq-like RNA chaperone YmaH. In *E. coli*, the small antisense RNA RyhB promotes the degradation of the mRNAs for several iron-binding and iron-storage proteins (25). This degradation is dependent upon RNase E, which cleaves double-stranded RNA, and the RNA chaperone Hfq. We therefore wondered whether RatA function is similarly dependent on an RNA chaperone. The *B. subtilis* genome contains an *hfq* ortholog called *ymaH*. We built a null mutant of *ymaH* and observed no defect in growth or sporulation (data not shown). We conclude that the interaction of RatA with *txpA* mRNA does not depend on an RNA chaperone or at least not on a chaperone with close similarity to Hfq. The related bacterium, *Listeria monocytogenes*, also contains an *hfq* ortholog which when mutant does not result in a growth defect but does impair the response to various stress conditions (8). A *B. subtilis* equivalent to RNase E that could be responsible for degrading *txpA*-RatA hybrids is not yet known.

Implications. In summary, we have identified a toxin-antitoxin system in *B. subtilis* in which the antitoxin is a small, untranslated RNA. The toxin gene *txpA* and the antitoxin gene *ratA* are in convergent orientation and overlap by ca. 75 bp at their 3′ ends. Evidence presented here indicates that RatA is an antisense RNA that likely anneals to the mRNA for TxpA and causes it to be degraded. Thus, RatA protects *B. subtilis* from TxpA by blocking the production of the toxin.

What is the biological function of the *txpA-ratA* module? A possible clue is provided by the fact that the gene pair is found in a 48-kb, phage-like element known as *skin*. The *skin* element interrupts the coding sequence for the mother-cell-specific regulatory protein σ^K during sporulation (22). The *skin* element is excised as a circle in a developmentally regulated manner from the chromosome in the mother cell compartment of the developing sporangium to create the intact coding sequence for σ^K. The element is not excised, however, from the chromosome in the forespore compartment. The mother cell is in effect a terminally differentiating cell type that nurtures the developing spore but is ultimately discarded by lysis. The forespore, on the other hand, is a germ line cell that gives rise to the mature spore and hence to future progeny. Thus, *skin* is retained in the

germ line even though it undergoes excision from the mother-cell chromosome during each round of spore formation. The *skin* can therefore be considered to be a selfish element that *B. subtilis* has been forced to retain in a functional state in order for spore formation to take place. Seen in this light, the *txpA-ratA* gene pair may function in a similar manner to the addiction modules of certain plasmids, helping to further ensure that *B. subtilis* cannot easily shed the *skin* element from its genome.

ACKNOWLEDGMENTS

We thank the members of the Losick laboratory and, in particular, D. Kearns, M. Fujita, and C. Ellermeier for helpful advice and discussions. We thank M. Kawano for kindly providing 5′- and 3′-RACE protocols. We also thank Jian-ming Lee for microarray analysis of *B. subtilis*.

This study was supported by NIH grant GM18568 to R.L.

REFERENCES

1. **Argaman, L., R. Hershberg, J. Vogel, G. Bejerano, E. G. Wagner, H. Margalit, and S. Altuvia.** 2001. Novel small RNA-encoding genes in the intergenic regions of *Escherichia coli*. Curr. Biol. **11:**941–950.
2. **Balaban, N. Q., J. Merrin, R. Chait, L. Kowalik, and S. Leibler.** 2004. Bacterial persistence as a phenotypic switch. Science **305:**1622–1625.
3. **Bensing, B. A., B. J. Meyer, and G. M. Dunny.** 1996. Sensitive detection of bacterial transcription initiation sites and differentiation from RNA processing sites in the pheromone-induced plasmid transfer system of *Enterococcus faecalis*. Proc. Natl. Acad. Sci. USA **93:**7794–7799.
4. **Bernhardt, T. G., I. N. Wang, D. K. Struck, and R. Young.** 2002. Breaking free: "protein antibiotics" and phage lysis. Res. Microbiol. **153:**493–501.
5. **Brantl, S.** 2002. Antisense RNAs in plasmids: control of replication and maintenance. Plasmid **48:**165–173.
6. **Brantl, S.** 2002. Antisense-RNA regulation and RNA interference. Biochim. Biophys. Acta **1575:**15–25.
7. **Christensen, S. K., K. Pedersen, F. G. Hansen, and K. Gerdes.** 2003. Toxin-antitoxin loci as stress-response-elements: ChpAK/MazF and ChpBK cleave translated RNAs and are counteracted by tmRNA. J. Mol. Biol. **332:**809–819.
8. **Christiansen, J. K., M. H. Larsen, H. Ingmer, L. Sogaard-Andersen, and B. H. Kallipolitis.** 2004. The RNA-binding protein Hfq of *Listeria monocytogenes*: role in stress tolerance and virulence. J. Bacteriol. **186:**3355–3362.
9. **Engelberg-Kulka, H., and G. Glaser.** 1999. Addiction modules and programmed cell death and antideath in bacterial cultures. Annu. Rev. Microbiol. **53:**43–70.
10. **Gerdes, K.** 2000. Toxin-antitoxin modules may regulate synthesis of macromolecules during nutritional stress. J. Bacteriol. **182:**561–572.
11. **Gerdes, K., S. K. Christensen, and A. Lobner-Olesen.** 2005. Prokaryotic toxin-antitoxin stress response loci. Nat. Rev. Microbiol. **3:**371–382.
12. **Gerdes, K., A. P. Gultyaev, T. Franch, K. Pedersen, and N. D. Mikkelsen.** 1997. Antisense RNA-regulated programmed cell death. Annu. Rev. Genet. **31:**1–31.
13. **Greenfield, T. J., E. Ehli, T. Kirshenmann, T. Franch, K. Gerdes, and K. E. Weaver.** 2000. The antisense RNA of the par locus of pAD1 regulates the expression of a 33-amino-acid toxic peptide by an unusual mechanism. Mol. Microbiol. **37:**652–660.
14. **Guerout-Fleury, A. M., N. Frandsen, and P. Stragier.** 1996 Plasmids for ectopic integration in *Bacillus subtilis*. Gene **180:**57–61.
15. **Guerout-Fleury, A. M., K. Shazand, N. Frandsen, and P. Stragier.** 1995 Antibiotic-resistance cassettes for *Bacillus subtilis*. Gene **167:**335–336.
16. **Harwood, C. R., and Cutting, S. M.** 1990. Molecular Biological Methods for *Bacillus.* John Wiley & Sons, Inc., New York, N.Y.
17. **Hayes, F.** 2003. Toxins-antitoxins: plasmid maintenance, programmed cell death, and cell cycle arrest. Science **301:**1496–1499.
18. **Helmann, J. D.** 1995. Compilation and analysis of *Bacillus subtilis* sigma A-dependent promoter sequences: evidence for extended contact between RNA polymerase and upstream promoter DNA. Nucleic Acids Res. **23:** 2351–2360.
19. **Karmazyn-Campelli, C., L. Fluss, T. Leighton, and P. Stragier.** 1992. The *spoIIN279(ts)* mutation affects the FtsA protein of *Bacillus subtilis*. Biochimie **74:**689–694.
20. **Kawano, M., T. Oshima, H. Kasai, and H. Mori.** 2002. Molecular characterization of long direct repeat (LDR) sequences expressing a stable mRNA encoding for a 35-amino-acid cell-killing peptide and a *cis*-encoded small antisense RNA in *Escherichia coli*. Mol. Microbiol. **45:**333–349.
21. **Keren, I., D. Shah, A. Spoering, N. Kaldalu, and K. Lewis.** 2004. Specialized persister cells and the mechanism of multidrug tolerance in *Escherichia coli*. J. Bacteriol. **186:**8172–8180.
22. **Kunkel, B., R. Losick, and P. Stragier.** 1990. The *Bacillus subtilis* gene for the development transcription factor sigma K is generated by excision of a dispensable DNA element containing a sporulation recombinase gene. Genes Dev. **4:**525–535.
23. **Lee, J. M., S. Zhang, S. Saha, S. Santa Anna, C. Jiang, and J. Perkins.** 2001. RNA expression analysis using an antisense *Bacillus subtilis* genome array. J. Bacteriol. **183:**7371–7380.
24. **Loh, S. M., D. S. Cram, and R. A. Skurray.** 1988. Nucleotide sequence and transcriptional analysis of a third function (Flm) involved in F-plasmid maintenance. Gene **66:**259–268.
25. **Masse, E., F. E. Escorcia, and S. Gottesman.** 2003. Coupled degradation of a small regulatory RNA and its mRNA targets in *Escherichia coli*. Genes Dev. **17:**2374–2383.
26. **Pandey, D. P., and K. Gerdes.** 2005. Toxin-antitoxin loci are highly abundant in free-living but lost from host-associated prokaryotes. Nucleic Acids Res. **33:**966–976.
27. **Pedersen, K., and K. Gerdes.** 1999. Multiple *hok* genes on the chromosome of *Escherichia coli*. Mol. Microbiol. **32:**1090–1102.
28. **Pellegrini, O., N. Mathy, A. Gogos, L. Shapiro, and C. Condon.** 2005. The *Bacillus subtilis ydcDE* operon encodes an endoribonuclease of the MazF/PemK family and its inhibitor. Mol. Microbiol. **56:**1139–1148.
29. **Resnekov, O., and R. Losick.** 1998. Negative regulation of the proteolytic activation of a developmental transcription factor in *Bacillus subtilis*. Proc. Natl. Acad. Sci. USA **95:**3162–3167.
30. **van Ooij, C., and R. Losick.** 2003. Subcellular localization of a small sporulation protein in *Bacillus subtilis*. J. Bacteriol. **185:**1391–1398.
31. **Vogel, J., L. Argaman, E. G. Wagner, and S. Altuvia.** 2004. The small RNA IstR inhibits synthesis of an SOS-induced toxic peptide. Curr. Biol. **14:**2271–2276.
32. **Wach, A.** 1996. PCR-synthesis of marker cassettes with long flanking homology regions for gene disruptions in *Saccharomyces cerevisiae*. Yeast **12:**259–265.
33. **Youngman, P. J., J. B. Perkins, and R. Losick.** 1983. Genetic transposition and insertional mutagenesis in *Bacillus subtilis* with *Streptococcus faecalis* transposon Tn*917*. Proc. Natl. Acad. Sci. USA **80:**2305–2309.